A&A 380, 673–683 (2001)
DOI: 10.1051/0004-6361:20011471

Astronomy & Astrophysics

HI observations of the high-velocity cloud in the direction of M 92⋆

J. V. Smoker[1], R. S. Roger[2], F. P. Keenan[1], R. D. Davies[3], R. H. Lang[4], and B. Bates[1]

[1] Astrophysics and Planetary Science Division, Department of Pure and Applied Physics, The Queen's University of Belfast, University Road, Belfast, BT7 1NN, UK
[2] National Research Council of Canada, Herzberg Institute of Astrophysics, Dominion Radio Astrophysical Observatory, Penticton, B.C. V2A 6K3, Canada
[3] The University of Manchester, Jodrell Bank Observatory, Lower Withington, Macclesfield, Cheshire, SK11 9DL, UK
[4] Department of Physics and Astronomy, University of Wales, Cardiff, 5, The Parade, Cardiff, CF24 3YB, UK

Received 22 May 2001 / Accepted 16 October 2001

Abstract. We present wide-field neutral hydrogen (H I) Lovell telescope multibeam, and Dominion Radio Astrophysical Observatory H I synthesis observations, of the high velocity cloud (HVC) located in the general direction of the globular cluster M 92. This cloud is part of the larger Complex C and lies at velocities between ∼–80 and −130 km s^{-1} in the Local Standard of Rest. The Lovell telescope observations, of resolution 12 arcmin spatially and 3.0 km s^{-1} in velocity, fully sampling a 3.1°×12.6° RA–Dec grid, have found that this part of HVC Complex C comprises two main condensations, lying approximately north-south in declination, separated by ∼2° and being parallel to the Galactic plane. At this resolution, peak values of the brightness temperature and H I column density of ∼1.4 K and ∼5×10^{19} cm^{-2} are determined, with relatively high values of the full width half maximum velocity (FWHM) of ∼22 km s^{-1} being observed, equivalent to a gas kinetic temperature, in the absence of turbulence and geometric effects of ∼10 000 K. Each of these properties, as well as the sizes of the clouds, are similar in the two components. The DRAO observations, towards the Northern HVC condensation, are the first high-resolution H I spectra of Complex C. When smoothed to a resolution of 3 arcmin, they identify several H I intensity peaks with column densities in the range 4–7×10^{19} cm^{-2}. Further smoothing of these data to 6 arcmin resolution tentatively indicates that parts of the HVC consist of two velocity components, of similar brightness temperature, separated by ∼7 km s^{-1} in velocity, and with FWHM velocity widths of ∼5–7km s^{-1}. No IRAS 60 or 100 micron flux is associated with the M 92 HVC. Cloud properties are briefly discussed and compared to previous observations of HVCs.

Key words. ISM: clouds – ISM: individual objects: M 92 HVC – radio lines: ISM

1. Introduction

Since their discovery forty years ago (Münch & Zirin 1961), the nature of high velocity clouds (HVCs); be it Galactic, extragalactic, or a combination of the two, has remained a subject of debate. As has been stated on numerous occasions, critical to the solution of their origin is the determination of HVC distances, combined with measurements of cloud properties such as metallicities, pressures and temperatures. Recently, progress has been made on several fronts, with distances being estimated for a handful of HVCs (e.g. Wakker et al. 1998; van Woerden et al. 1999; van Woerden et al. 1999).

Send offprint requests to: J.smoker,
e-mail: j.smoker@qub.ac.uk

⋆ Based on observations made with the Lovell telescope, Jodrell Bank, UK, the Synthesis Telescope at the Dominion Radio Astrophysical Observatory, Canada, and at the Isaac Newton Group of telescopes, La Palma, Spain.

In order to put upper distance limits on HVCs, Galactic halo stars are often used as probes with which to search for HVC absorption; the presence of such an interstellar absorption indicates that the cloud must be closer than the stellar distance. One obvious location for such halo stars is within globular clusters, and hence Kerr & Knapp (1972) (hereafter KK72) searched for high velocity H I towards a number of such objects. Historically, an actual physical association between HVCs and globular clusters has also occasionally been postulated (Shatsova 1983), based upon the similarity in the radial velocities of the two types of objects (Lynden-Bell 1976), although recent work has ruled out such an association (Wakker & van Woerden 1997).

KK72 found high velocity gas at ∼–100 km s^{-1} within 1 degree of M 92, at a position of RA = 17$^{\rm h}$22$^{\rm m}$32$^{\rm s}$, Dec = +42°48′13″ (J2000); the study of this cloud is the subject of the current paper. The well-studied old globular cluster M 92 (RA = 17$^{\rm h}$17$^{\rm m}$07.27$^{\rm s}$, Dec = +43°08′11.5″ (J2000);

$l = 68.34°$, $b = +34.86°$) has a distance of ∼8.9 kpc (Carretta et al. 2000) which puts it in the upper Galactic halo with a distance from the disc (z) of 5.1 kpc.

From the low-resolution all sky Leiden/Dwingeloo survey (Hartmann & Burton 1997), the HVC located in the general vicinity of M 92 is known to extend over several square degrees. In fact, M 92 lies in the line of sight of one of the largest angular-diameter HVCs known, Complex C. Low and medium resolution observations towards parts of this cloud have previously been published by Giovanelli et al. (1973), Hulsbosch (1975) and Davies et al. (1976). These show the HVC to have a velocity in the Local Standard of Rest of ∼–100 to –160 km s^{-1} and brightness temperature at a resolution of ∼10 arcmin of ∼1 K. Complex C is thought to lie at a distance exceeding 6 kpc (van Woerden et al. 1999). Figure 1 shows the Leiden/Dwingeloo H I column density map in the vicinity of M 92, integrated from −120 to −85 km s^{-1} in the LSR, and only showing a part of Complex C, which covers a region of the sky approximately bounded by $65° < l < 135°$ and $30° < b < 55°$. Complex C is comprised of small condensations of material with characteristic sizes of less than ∼30 armin, immersed in extended areas with a diffuse appearance, and showing no obvious pattern in velocity structure for the different parts of the complex (Giovanelli et al. 1973). The area observed by the current multibeam observations is also shown on the figure, showing how the mapped area covers two of these condensations, which at half-degree resolution have peak H I column densities ($N_{\rm HI}$) of $\sim 4\times10^{19}$ cm^{-2}.

Before the advent of multibeam systems combined with low-noise receivers, the mapping of such an extended object at 12 arcmin resolution with full sampling would have been a large undertaking. However, with the new 4-beam system on the 76-m Lovell radio telescope, obtaining a datacube of several square degrees in the general direction of M 92 proved to be relatively straightforward.

The current paper is the third of a series of observations of isolated H I clouds in the vicinity of globular clusters; previously intermediate velocity (IV) gas towards both M 13 and M 15 (Shaw et al. 1996; Kennedy et al. 1998) has been mapped in H I using a combination of the Lovell telescope plus synthesis data. In particular, the M 13 observations were also towards Complex C, although in this case for an intermediate velocity cloud, which may or may not be associated with the main HVC in this region. Aside from obtaining upper limits to cloud distances (in combination with absorption-line spectroscopy), these observations also allow information to be derived on cloud properties such as masses, sizes, column densities, temperatures and abundances, which provide clues to the cloud's origin and current environment. Cloud properties are often found to be a function of spatial resolution. Hence in order to obtain high-resolution data towards a region of the current cloud, we also describe here Dominion Radio Astrophysical Observatory H I synthesis observations of a part of the M 92 HVC, albeit of lower sensitivity than the Lovell telescope observations. Previous arcminute-scale observations of IVCs and HVCs have found that typically these objects are clumpy with peak values of brightness temperature increasing with resolution (e.g. Complex A: Schwarz & Oort 1981; M 13 IVC: Shaw et al. 1996; CHVC125+41–207: Braun & Burton 2000; M 15 IVC: Smoker et al. 2001). Hence a priori we expected to see structure on finer scales.

Section 2 details the observations and data reduction, Sect. 3 gives the results, Sect. 4 contains the discussion and Sect. 5 gives a summary and the conclusions.

2. Observations and data reduction

2.1. Lovell telescope 21-cm H I multibeam observations

The Lovell telescope 21-cm H I observations presented in this paper were taken during parts of four nights from 31 May 2000 to 3 June 2000; observational details are shown in Table 1. The "narrow-band" multibeam system was used, which has four independent beams and eight receiver systems. For these observations a bandwidth of 8 MHz was in place; over the 1024 channels of each of the correlators, the resulting channel width was 1.649 km s^{-1}, which corresponds to a velocity resolution of ∼3.0 km s^{-1}. Online calibration was performed via frequent firing of a noise diode. Because the backend control software was in a preliminary state, a fixed local oscillator was used with no corrections being applied for the motion of the Earth through space. Hence, over the course of the observations, the correction to the Local Standard of Rest (LSR; Allen 1973), estimated using the program RV (Wallace & Clayton 1996), varied by ∼0.3 km s^{-1}. As the velocity width of the HVC is quite high, we simply applied an average LSR correction to the data a posteriori.

The observations were obtained by first performing scans of an RA–Dec grid of size $\sim 3.1°\times12.6°$, centred upon RA = $17^{\rm h}20^{\rm m}46^{\rm s}$, Dec = $+42°00'30''$ (J2000). This provided beams named a–d. Finally, the whole grid was again scanned but this time with an offset of 0.1° in RA from the first set of integrations. This provided beams e–h. When combined, the beams a–h provide a fully–sampled grid of positions covering the M 92 HVC.

Data were initially reduced and a datacube made using the LIVEDATA and GRIDZILLA packages (Barnes et al. 2001) within AIPS^{++}. These programs act to remove the bandpass response from each of the individual beam spectra and then combine the bandpass-subtracted spectra. For the baseline subtraction, an average of the spectra at the extreme 3 degrees to the North and South of the field was derived by LIVEDATA; this baseline was subtracted from the central 6 degree declination strip. Outside of this strip, there is signal of ∼0.07 K visible at a resolution of 0.5° (Hulsbosch & Wakker 1988) that will cause a systematic uncertainty in the baseline level at the HVC velocity. An example of a resulting baseline-subtracted spectrum produced by LIVEDATA is displayed in Fig. 2. The flatness of the derived spectra is reassuring, with the baseline removal only failing at the edges of the band and,

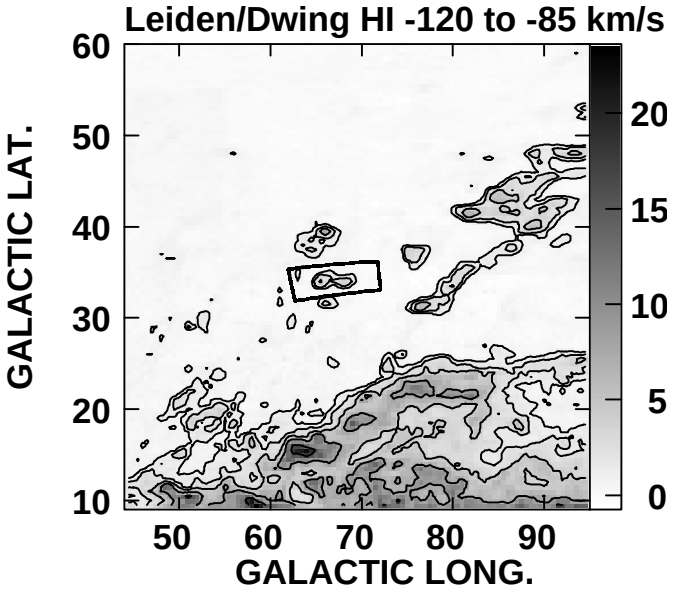

Fig. 1. Leiden/Dwingeloo H I column density map towards a part of Complex C, integrated from −120 to −85 km s^{-1} in the LSR and of resolution 30 arcmin. The area mapped by the current multibeam observations (centred on $l \sim 67°$, $b \sim 34°$) is enclosed by a rectangle. Contour levels are at (1, 2, 4, 8, 16)×10^{19} cm^{-2}, with the Greyscale from 0−24×10^{19} cm^{-2}.

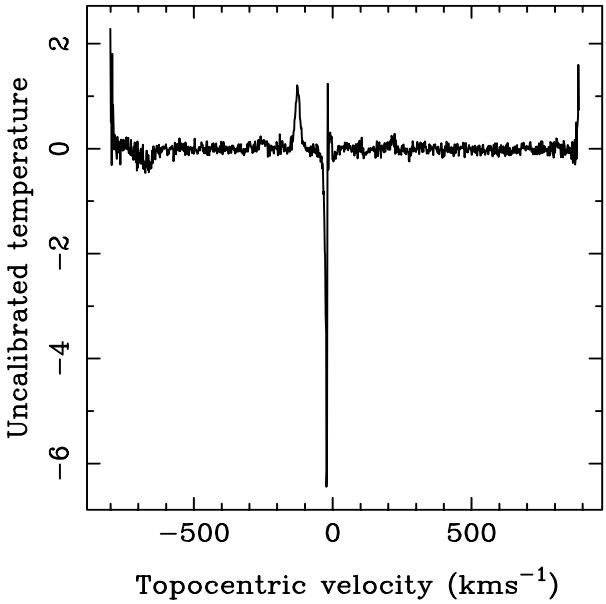

Fig. 2. Example of a "raw" baseline-corrected spectrum towards the M 92 HVC, in uncalibrated flux units, plotted against observed (topocentric) velocity. The HVC is visible at a velocity of ∼−120 km s^{-1}. The negative-temperature spike at ∼0 km s^{-1} is caused by the baseline-removal algorithm.

predictably, around zero velocity where there is of course no "blank" region of the sky to act as a template spectrum. Clearly, for low velocity (LV) gas the current procedure is not appropriate, and thus we have no information concerning the LV component as is obtained by more conventional (and time-consuming) baseline-removal algorithms.

Because of the type of baseline-removal applied and the resulting lack of any low-velocity gas in our final spectra, calibration of the multibeam data was performed by use of previous Lovell telescope observations. These were taken on two different days in April 1996, and are of the Kerr & Knapp (1972) position near to the M 92 globular cluster, plus another region where the HVC is somewhat fainter, hereafter named "P1" (RA = 17$^{\rm h}$23$^{\rm m}$01$^{\rm s}$, Dec = +43°13′37″, J2000).

These 1996 observations were calibrated in terms of the standard region S7 ($l = 132.0°$, $b = –0.99°$) which was assumed to have a peak brightness temperature, including stray radiation, of 108 K (Kalberla et al. 1982). Using this calibration, the Kerr & Knapp (1972) position was found to have a peak HVC brightness temperature value at the Lovell-telescope resolution of 1.08 K and brightness temperature integral, integrated from an LSR velocity of –130 km s^{-1} to –60 km s^{-1}, of 27.4 K km s^{-1}; the corresponding values for P1 were 0.65 K and 11.0 K km s^{-1}. The LSR velocity at the KK72 position was –99 km s^{-1} with a FWHM velocity width of 24.4 ± 0.6 km s^{-1} which compares with a value of 22.3 ± 0.6 km s^{-1} for the current observations.

By comparing the uncalibrated multibeam peak temperature and temperature integral for these positions with the values derived above, we obtained the calibration factor to convert to brightness temperature ($T_{\rm B}$) for the whole datacube. We estimate the accuracy of this calibration to be ∼15 per cent. Figure 3 shows plots of the 1996 single-dish Lovell telescope $T_{\rm B}$ spectra overlaid on the current multibeam observations both at the centre of M 92 and also towards the two regions used for purposes of calibration.

After calibration had been undertaken, final analysis was performed within the program AIPS[1]. This included moments analysis of the datacube from –120 km s^{-1} < $V_{\rm LSR}$ < –85 km s^{-1}, estimated from data with $T_{\rm B} > 0.2$ K, and finally conversion into H I column density values via;

$$N_{\rm HI} = 1.823 \times 10^{18} \int T_{\rm B} {\rm d}v \ {\rm cm}^{-2}, \quad (1)$$

where v is the velocity in km s^{-1}.

2.2. DRAO 21-cm H I synthesis observations

The high-resolution observations described in this paper were taken using a full synthesis run during August 1998 with the synthesis telescope at the Dominion Radio Astrophysical Observatory[2] (Landecker et al. 2000). Because of the relatively small size of the antennae combined with the excellent UV-coverage, this telescope has a

[1] AIPS is distributed by the National Radio Astronomy Observatory, USA.

[2] The DRAO Synthesis Telescope is operated as a national facility by the National Research Council of Canada.

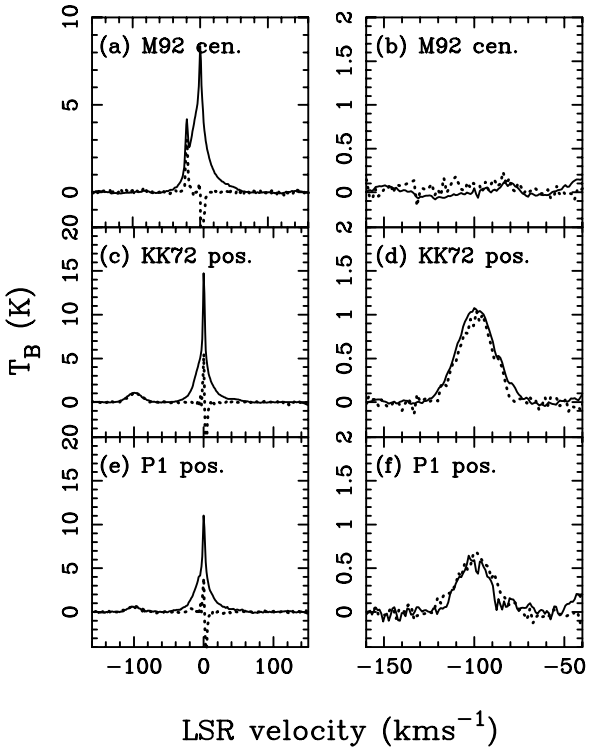

Fig. 3. Plots of Lovell telescope brightness temperature H I spectra taken in 1996 (solid line) overlaid by the current multibeam data at the same position (dotted line). Panels **a)** and **b)** depict the observations towards M 92 (RA = $17^{\rm h}17^{\rm m}07^{\rm s}$, Dec = $+43°08'11''$); panels **c)** and **d)** present the corresponding spectra at the Kerr & Knapp (1972) position (RA = $17^{\rm h}22^{\rm m}32^{\rm s}$, Dec = $42°48'13''$); panels **e)** and **f)** are towards position P1 (RA = $17^{\rm h}23^{\rm m}01^{\rm s}$, Dec = $+43°13'37''$). The equinox is J2000.

large field of view and good sensitivity to large-scale structure. However, the minimum spacing in the interferometer is ∼61 λ (EW), so the synthesized maps do not represent structure on a scale of greater than ∼30 arcmin. Flagging and inversion of the visibility data were performed by observatory staff. The inverted data were cleaned using APCLN within AIPS. The velocity and spatial resolution of the mapped data were 0.82 km s^{-1} and $86''\times57''$ respectively. A continuum image was constructed from 30 line-free channel maps and was subtracted from the line datacube after which conversion into brightness temperature from flux density in mJy was performed using $T_{\rm B}({\rm K}) = S_{\rm mJy}/5.86$. At the map centre, the rms noise in the cleaned maps (at a channel width of 0.82 km s^{-1}) was 2.8 K, compared with the theoretical value of 2.3 K. Unfortunately, because the Lovell telescope multibeam observations were taken after the DRAO data, the position of the peak H I strength was unknown a priori and turned out to be some ∼0.7 degrees from the pointing centre, where the noise was 50 per cent higher. Hence, in order to improve the signal-to-noise, the cube was convolved within AIPS to form maps of spatial resolution 3, 6 and 12 arcmin. Moments analysis was then performed between –120 and –85 km s^{-1} on the cube of 3 arcmin resolution to produce the H I column density maps where the signal exceeded 0.9 K. Finally, these maps were primary beam corrected within AIPS using an assumed function of $(\cos^6(30.24\times{\rm radius\ in\ degrees}))^{-1}$ (Landecker et al. 2000).

2.3. INT IDS Ca II optical spectroscopy

In order to search for interstellar absorption components due to the HVC at ∼–100 km s^{-1}, Ca II K observations towards a cluster star within M 92 (XII–1; RA = $17^{\rm h}17^{\rm m}44.5^{\rm s}$, Dec = $+43°06'00''$, J2000) were obtained during August 1999 using the Intermediate Dispersion Spectrograph on the Isaac Newton Telescope, providing an instrumental resolution of ∼0.5 Å, equivalent to ∼40 km s^{-1} at this wavelength. This star was chosen as there is an indication in Greenstein (1968) that HVC absorption was seen towards this object. Observational details and data reduction procedures are discussed in Smoker et al. (2001).

Figure 4 displays the observed Ca II K spectrum ($\lambda\lambda$ = 3933.66 Å) towards this star shifted to the LSR. Twin component Gaussian-fitting to this profile reveals that the stellar line is located at ∼–115 km s^{-1} and has an equivalent width (EW) of 0.92 ± 0.07 Å, corresponding to an early A-type star (Jaschek & Jaschek 1987). This compares with the Greenstein (1968) result of EW(Ca II K) = 0.7 Å. The weaker interstellar feature, caused by low-velocity gas, is centred on ∼–15 km s^{-1} and has EW = 0.21 ± 0.05 Å. This compares to the canonical value, which has a large scatter, of $EW \sim 0.2$ Å for the Ca II K line integrated perpendicular to the Galactic plane (Beers 1990). We note that using observations of the Na I D lines, Langer et al. (1990) and Andrews et al. (2001) found two low-velocity components towards the centre of M 92, at LSR velocities of ∼0 and −19 km s^{-1}, although no HVC absorption. In our Ca II spectra, no obvious interstellar HVC components are visible, perhaps not surprising given that the main HVC condensation is located away from the M 92 core, the stellar lines are strong, and the HVC and globular cluster velocities are similar. However, it remains a possibility that the observed profile is a superposition of high velocity interstellar and stellar components. Higher-resolution observations could determine whether this is the case or not, although this would be challenging.

2.4. IRAS ISSA survey archive data retrieval

In order to search for IRAS emission from the M 92 HVC, we extracted the 60 and 100 micron images of the M 92 field from the on-line versions of the IRAS Sky Survey Atlas (ISSA). These images are of resolution ∼5 arcmin and have most of their zodiacal emission removed, although they have an arbitrary zero-point. There was no correlation observed between the HVC H I column density map and IRAS images, in common with previous observations of HVCs (Wakker & Boulanger 1986). This is unsurprising; using an $I(100\ \mu)/N({\rm H\,I})$ ratio of 0.6 MJy/sr/10^{20} cm^{-2} appropriate to low-velocity gas

Table 1. Details of the Lovell telescope H I multibeam and DRAO H I synthesis observations towards the M 92 HVC.

Telescope	Lovell multibeam	DRAO synthesis telescope
Observing dates	31 May 2000 to 3 June 2000	August 1998
Observing time	18 hours	12×12 hours
Field centre (J2000)	RA = $17^h20^m46^s$, Dec = $+42°00'30''$	RA = $17^h19^m50^s$, Dec = $+42°58'12''$
Field centre (Galactic coords)	$l = 67.08°$, $b = +34.05°$	$l = 68.21°$, $b = +34.35°$
Field size	3.1°×12.6° (RA–Dec)	FWHM of primary beam ∼107 arcmin
Bandwidth (MHz)	8.0	1.0
Number of channels	1024	256
Channel width (km s^{-1})	1.65	0.82
Beamsize	12′	86″×57″ (NS×EW)
rms noise channel^{-1} (K)	0.06	2.8

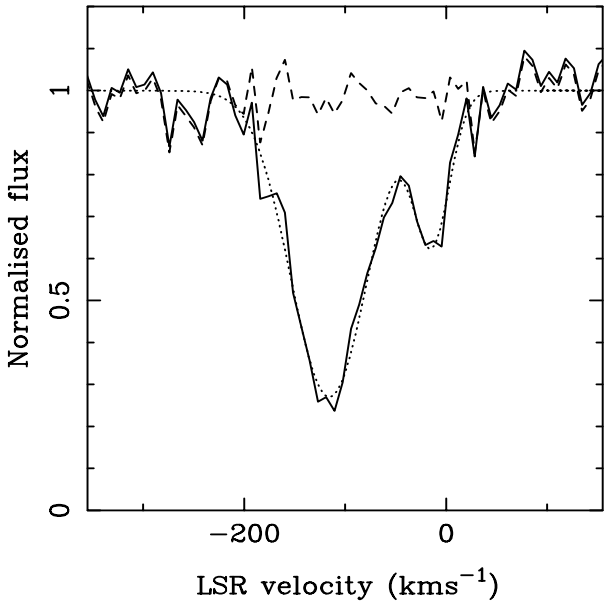

Fig. 4. INT IDS Ca II K spectrum towards the globular cluster star M 92 XII-1, showing the stellar line at ∼–115 km s^{-1} and low velocity interstellar absorption at ∼–15 km s^{-1}. The dotted line indicates a two-component Gaussian fit and the dashed line the (data−fit) residual. No obvious HVC component is visible.

(Boulanger et al. 1996), combined with a detection limit of ∼0.1 MJy sr^{-1}, even the cloud H I column density peaks would only be 3σ detections were there the same gas-to-dust ratio in the HVC. Generally, lack of detection argues for a lower $I(100\ \mu)/N(\mathrm{H\,I})$ ratio, or cooler dust because of there being a less intense radiation field due to the distance of the HVC from the Galactic plane.

3. Results

3.1. Lovell telescope 21-cm H I multibeam results

Table 2 shows the H I parameters derived from the current observations, with Fig. 5 showing the Lovell telescope H I channel maps for the M 92 high velocity cloud. Two main clumps of gas are evident, hereafter called the N (for North) and S (for South) clouds. In the following, we assume that the clouds lie at the same distance, due to the fact that there is detectable gas between them, although of course this could just be a line-of-sight effect. At LT resolution, the N and S cloud have similar values for their peak T_B values (1.2 K and 1.4 K respectively), with the temperature profiles at these positions being depicted in Fig. 6. Both profiles are reasonably well-fitted by a Gaussian, with no obvious two-component (narrow and broad) structure visible, although at the velocity resolution of the current data (∼3 km s^{-1}), a weak and narrow component may remain undetected. At these two positions within the HVC, the FWHM velocity widths (measured using the program DIPSO; Howarth et al. 1996) are 22.0 ± 0.7 and 21.5 ± 0.7 km s^{-1}. Assuming that turbulence is negligible, and that the observed profile is not simply made up of a number of gas clouds of different velocities superposed in the line-of-sight (which may not be the case for cloud N, as discussed in Sect. 3.2), these widths correspond to a kinetic temperature of the gas of $\sim 10^4$ K. With non-negligible turbulence, this temperature is an upper limit. Figures 7 and 8 show the H I spectra for the S cloud and N cloud, respectively. As can be seen, a Gaussian fit is appropriate to the S cloud as a whole. This compares with the N cloud where the position RA = 17^h19^m, Dec = $+42°40'$ shows a flat-topped profile, indicating possible superposition of components, although the signal to noise of the data are low. Possible multicomponent structure was infact tentatively detected by the DRAO observations (see Sect. 3.2).

Figure 9a displays the Lovell telescope M 92 HVC H I column density map overlaid on the digital sky survey image. The limiting column density of these observations for this HVC (FWHM ∼ 20 km s^{-1}) is ∼0.5–1.0×10^{19} cm^{-2}. At this resolution, both the N and S clouds are quite smooth. The major axis of the whole cloud lies parallel to the Galactic plane, although of course the current map only samples a part of Complex C, and by chance some of its components will be aligned with the plane. Peak values of the column density are around 5×10^{19} cm^{-2} in both the Northern and Southern clouds. Changes in H I column density towards the clouds edges of a factor ∼5 occur over distances of ∼20 arcmin (corresponding to ∼60 pc for an assumed distance of 10 kpc), in both clouds N and S.

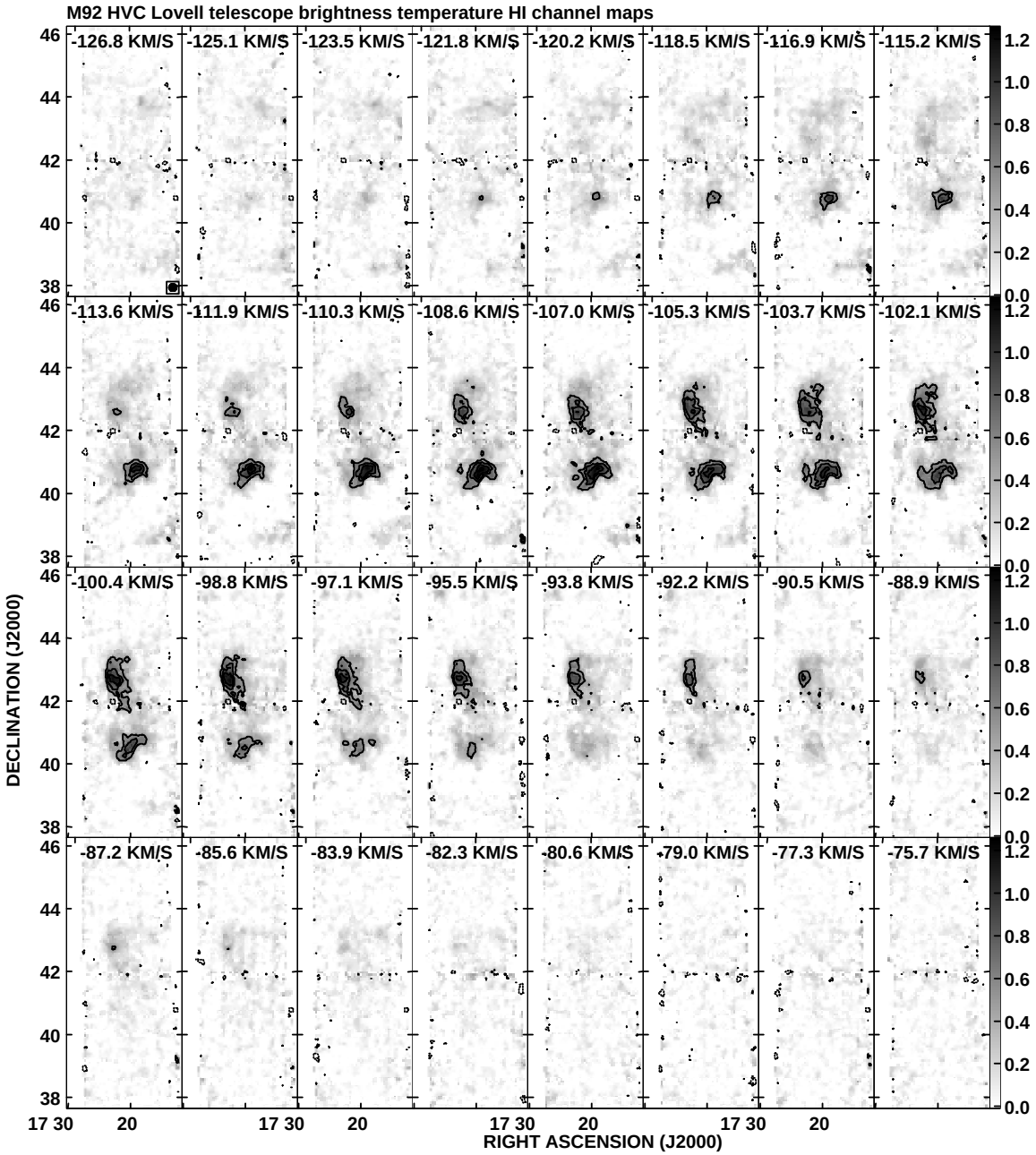

Fig. 5. Lovell telescope H I channel maps towards the M 92 HVC. Velocities are in the LSR. Brightness temperature contours are at (–0.25, 0.25, 0.5, 0.75, 1.0, 1.25) K, with greyscale levels from 0 to 1.25 K.

If the gas geometry is filamentary or spherically symmetric (and not in some sheet-like form; Heiles 1997), then using the size of the clouds at full-width half maximum intensity (∼0.55 and 0.45 degrees for N and S components, respectively) results in a H I volume density, at an assumed distance (D) of 10 kpc, of $0.17/(D)$ cm^{-3} and $0.22/(D)$ cm^{-3} for components N and S, respectively.

The velocity fields of the M 92 HVC, derived using moments analysis, are shown in Fig. 9b, and for the two cloudlets are somewhat different. Aside from the mean velocities of the clouds being displaced by ∼5 km s^{-1} with respect to each other, cloudlet N does not show any particular velocity gradient with position, whereas S displays a distinctive gradient. This is depicted in Fig. 9c, which shows slices in velocity across both the southern and northern clouds. If we now consider the velocity widths of the two clouds at a resolution of 12 arcmin, they are again quite similar. Single-component Gaussian fitting using XGAUS within AIPS of all features with successive channels with $T_{\rm B} > 0.5$ K reveals that for the S cloud there is a mean FWHM = 21.5 km s^{-1} with standard deviation of 1.4 km s^{-1}; for cloud N the corresponding values are 23.0 km s^{-1} and 2.4 km s^{-1}.

If the S and N clouds consist of a single Gaussian component, then the kinetic energies of the H I towards the clouds is given by $U = 1.5 \times NkT$, where T is the cloud "temperature" (corresponding to the sum of the thermal and turbulent motions), k is Boltzmann's constant and N

Table 2. H I results for the Northern and Southern components of the M 92 HVC observed with the Lovell telescope at a resolution of 12 arcmin. Additionally, DRAO synthesis H I results, at a resolution of 3 arcmin, for the peaks (a)−(d) within the Northern cloud are shown. Values of the peak H I column density for the DRAO data are derived from both moments analysis and single-component Gaussian fitting (in brackets). Note that the FWHM velocity widths are uncertain, at least in the Northern cloud, due to possible two-component velocity structure (see text). Cloud masses and sizes are estimated assuming a distance of 10 kpc.

	Whole Cloud Res. = 12′	Cloud N Res. = 12′	Cloud S Res. = 12′	(a) Res. = 3′	(b) Res. = 3′	(c) Res. = 3′	(d) Res. = 3′
H I mass ($M_\odot \times D^2_{10\mathrm{kpc}}$)	17 000	9000	8000	–	–	–	–
Size (degrees at N_{HI}=10^{19} cm^{-2})	Maj. axis 3.0	1.4×0.7	1.2×0.7	–	–	–	–
Size (degrees at FWHP)	–	1.2×0.6	0.9×0.5	–	–	–	–
Size (kpc×$D_{10\mathrm{kpc}}$ at 10^{19} cm^{-2})	Maj. axis 0.52	0.25×0.12	0.21×0.12	–	–	–	–
Peak H I col. dens. (×10^{19} cm^{-2})	5.1	4.8	5.1	5 (7)	5 (6)	4 (5)	4 (6)
Peak T_{B} value (K)	1.4	1.2	1.4	3.4	2.4	2.6	2.5
LSR velocity (km s^{-1})	–103.4 ± 3.6	–100.9 ± 2.0	–106.5 ± 2.3	–100.8 ± 0.6	–99.1 ± 0.9	–96.5 ± 1.1	–101.3 ± 0.8
FWHM velocity (km s^{-1})	22.3 ± 2.3	23.0 ± 2.4	21.5 ± 1.4	16.2 ± 2.3	20.5 ± 2.7	20.3 ± 3.2	18.1 ± 3.1

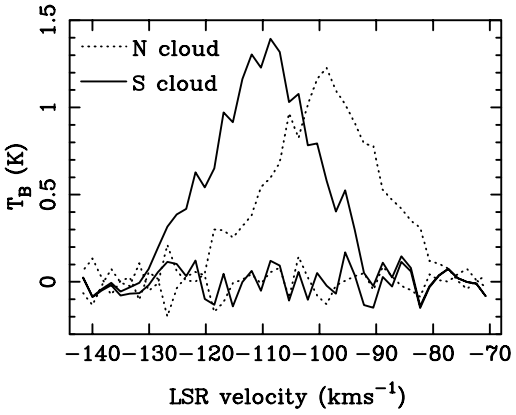

Fig. 6. Lovell telescope H I brightness temperature profiles towards the regions of peak T_{B} in the Northern and Southern components of the M 92 HVC. The lines around $T_{\mathrm{B}} = 0$ are the residuals from a (single Gaussian model)–data fit for each peak. The velocity centroids and FWHM values are -99.0 ± 0.3 km s^{-1}, 22.0 ± 0.7 km s^{-1} for cloud N and -109.7 ± 0.3 km s^{-1}, 21.5 ± 0.8 km s^{-1} for cloud S.

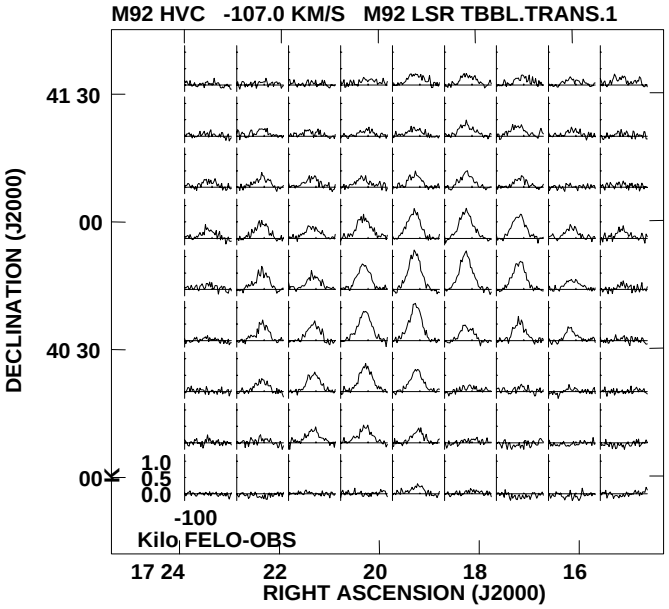

Fig. 7. Lovell telescope H I brightness temperature profiles towards the Southern part of the M 92 HVC showing their Gaussian nature. Spectra are plotted each beamwidth (12 arcmin).

are the number of hydrogen atoms in the neutral state. At an assumed distance of 10 kpc, the S and N clouds have KE of ≈2×10^{42} Joules. The potential energy of each cloud is –0.6×GM^2_{HI}/R, or ≈–4×10^{40} Joules, where G is the gravitational constant, R is the cloud radius and M_{HI} is the clouds H I mass. Hence, in the absence of large quantities of dark matter, constraining magnetic fields or a confining hot intergalactic medium, and assuming the cloud is not at local group distances, the clouds are unbound; typical of other studies of IVCs and HVCs.

Figure 13 shows the H I data from the current multibeam observations, and also higher-sensitivity single-beam 1996 Lovell telescope observations towards the globular cluster M 92. The figure also displays Leiden/Dwingeloo survey H I spectra (Hartmann & Burton 1997) from the nearest four positions to M 92 ($l = 68.34°$, $b = 34.86°$). The current multibeam observations are of insufficient sensitivity to detect high-velocity H I towards M 92. The earlier LT observations *appear* to detect H I towards the cluster, with central velocities of ∼–148 km s^{-1} and ∼–84 km s^{-1}, peak brightness temperatures of ∼0.1 K, and brightness temperature integrals of ∼2 ± 1 K km s^{-1}, corresponding to $N_{\mathrm{HI}} \sim 3.5 \times 10^{18}$ cm^{-2}. A component in the $l = 68.0°$, $b = 34.5°$ Leiden/Dwingeloo spectrum at ∼–145 km s^{-1} is also detected. However, the other higher-velocity component at this position is centred upon ∼–103 km s^{-1}, offset by some ∼20 km s^{-1} from the 1996 Lovell telescope velocity, and casting doubt on the Lovell telescope result. Further spillover-corrected, high-sensitivity observations would be useful to clarify this point.

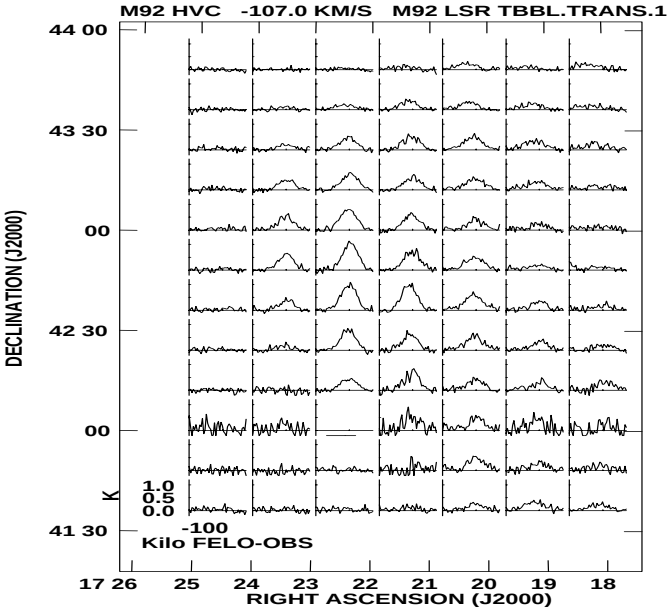

Fig. 8. Lovell telescope H I brightness temperature profiles towards the Northern part of the M 92 HVC. Spectra are plotted each beamwidth (12 arcmin).

3.2. DRAO 21-cm H I synthesis results

Figure 10 shows the DRAO H I column density map smoothed to a resolution of 3 arcmin superimposed upon the Lovell telescope data. As noted in Sect. 2.2, these synthesis maps are only sensitive to structures on scales smaller than ∼30 arcmin. The half power beamwidth of the primary beam at this frequency is ∼107 arcmin, although as noted by Landecker et al. (2000), the usable field of view can extend beyond this. At the DRAO resolution, the cloud is shown to contain several peaks not seen in the Lovell telescope data alone. The peak column density derived using moments analysis is $N_{\rm HI} \sim 7{\times}10^{19}$ cm^{-2}, some 20 per cent higher than that observed with the single-dish data. The peak $T_{\rm B}$ value is ∼3 K. Figure 11 shows the $T_{\rm B}$ spectra at the positions of the four brightest peaks in the DRAO H I column density map smoothed to 3 and 6 arcmin resolution.

At 3 arcmin resolution, the clumps (a)–(d) have FWHM values of between 16–20 ± 3 km s^{-1}, similar to the lower-resolution Lovell telescope results. However, there is a hint of a two-component structure in the velocity profile, which warrants further investigation as the signal-to-noise of the current observations is quite low. Smoothing of the current data to a resolution of 6 arcmin *does* indicate that two-component velocity structure is present, particularly towards clump (a). Figure 12 displays the observed data and two-component fit towards clump (a); here there are two main velocity peaks at $-98.0{\pm}0.4$ km s^{-1} and -105.0 ± 0.4 km s^{-1} with FWHM widths of 4.5 ± 1.5 km s^{-1} and 6.5 ± 2.0 km s^{-1} respectively and brightness temperatures of ∼1.5 K. Towards Complex C, this is not an unexpected finding, as previous low and intermediate-resolution observations have indicated that there are several velocity components present (Hulsbosch 1975; Davies et al. 1976).

4. Discussion

The position and LSR velocity of the centre of the M 92 HVC (∼l = 67°, b = +34°) make it a part of Complex C, which is in turn part of the large complex of Northern Hemisphere clouds (cf. Fig. 1f of Wakker & van Woerden 1991).

Complex C remains one of the few HVC groupings with a relatively well defined distance, lying in the range ∼5–25 kpc, although the upper distance limit is based on indirect evidence (van Woerden et al. 1999). It may be the case that the larger HVCs (such as Complex C) are nearby, with the compact high velocity clouds being at several tens of kpc in distance (Braun & Burton 2000). Of course, with few *direct* distance estimates thus far obtained, this remains speculative. Assuming a distance of 10 kpc, the current observations sample the M 92 cloud at resolutions of 9 pc and 35 pc, for beamsizes of 3 and 12 arcmin, respectively.

Taken as a whole, the observed properties of the M 92 HVC are similar to previous studies of such Northern objects observed at intermediate resolution. For example, both the current cloud, and also previous observed Northern-Hemisphere HVCs, have broad FWHM profiles, ranging from 20−30 km s^{-1}. We note that when HVCs are observed at higher resolution, it is often the case that values of FWHM markedly decrease. For the M 92 N cloud, at least at the current sensitivity, this also appears to be the case, with linewidths of ∼5 to 7 km s^{-1} being observed, similar to Northern Complexes A, H and M, which have FWHM values of 3–10 km s^{-1} at resolutions of 1–3 arcmin (Wakker & Schwarz 1991). If linewidths do *not* decrease, with increasing resolution, this behaviour is similar to that found in the Galactic anticentre clouds by Mirabel (1982), which show large linewidths (∼20–30 km s^{-1}) even at 3 arcmin resolution. Peak values of $N_{\rm HI}$ are also similar to previous observations of Northern hemisphere IVCs and HVCs at this resolution (e.g. Davies 1975; Cohen & Mirabel 1979; Shaw et al. 1996; Kennedy et al. 1998), which range from ∼3–5×10^{19} cm^{-2}.

The similarity between the N and S components of the cloud, in terms of angular size, H I mass, H I column density and velocity widths (all at the observed resolution of ∼12 arcmin, equivalent to ∼35 pc at D = 10 kpc), *may* tell us that the conditions in which they were formed and/or exist today are similar. Of course, to some extent this is dependent upon selection effects; for example, if either cloud has an extended halo of low density material it would remain undetected by the LT data. Similarly, the S cloud has not yet been observed at high resolution so its small-scale properties, such as linewidths and brightness temperatures, remain unknown.

With this caveat, there are only two marked differences between the N and S clouds. The first is the presence of a velocity gradient of ∼8 km s^{-1} across cloud S, corresponding to ∼12 km s^{-1} degree^{-1}. In cloud N, there

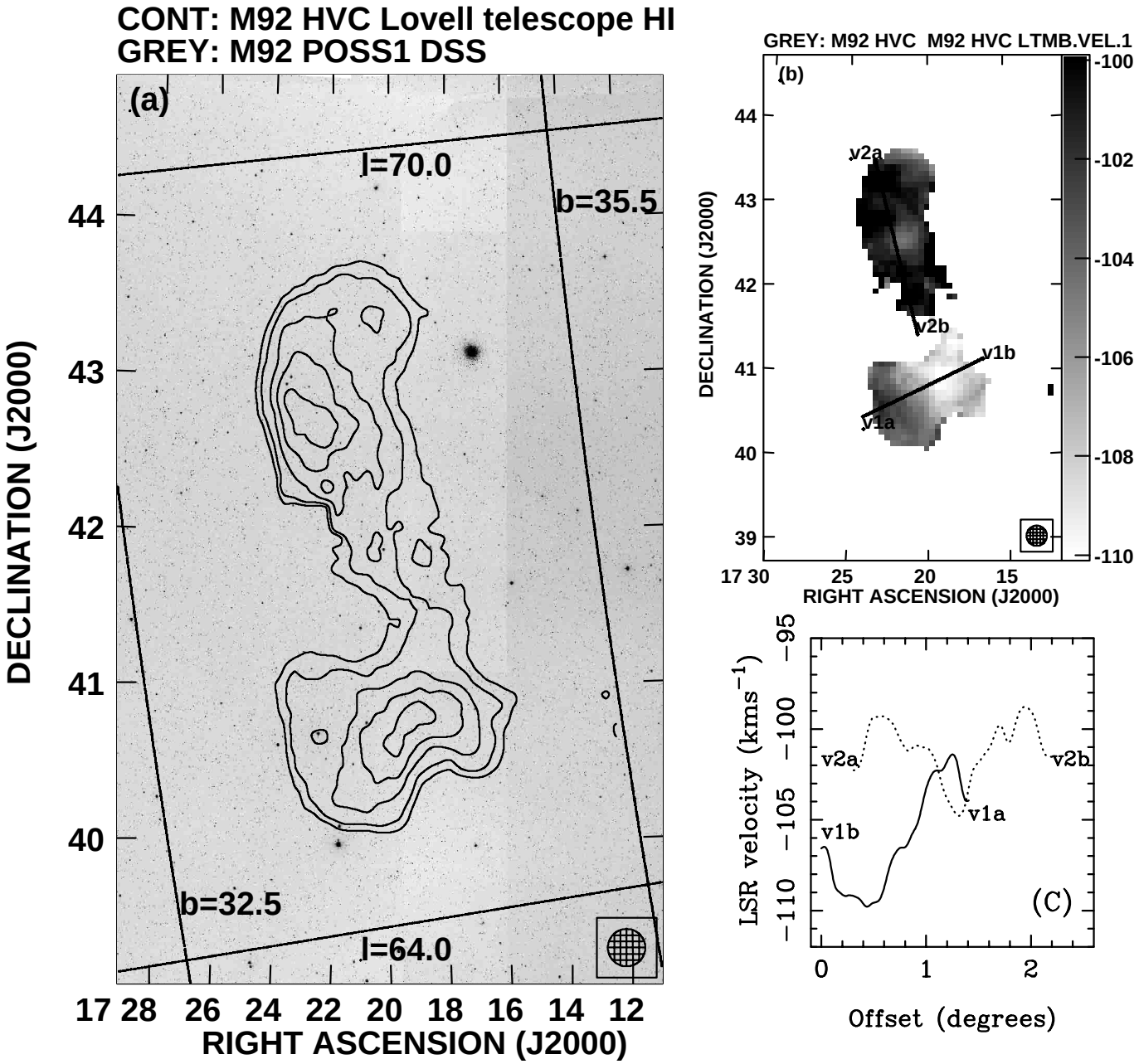

Fig. 9. a) Lovell telescope H I column density map of the M 92 HVC, integrated from -120 to -85 km s^{-1}, overlaid on the Digitised Sky Survey POSS1 image. Contour levels are at $N_{\rm HI} = (0.5, 1, 2, 3, 4) \times 10^{19}$ cm^{-2}. The M 92 globular cluster is at RA = $17^{\rm h}17^{\rm m}07.27^{\rm s}$, Dec = $+43^\circ08'11.5''$ (J2000). Lines of constant Galactic latitude and longitude are also displayed on the figure. **b)** Velocity field obtained using moments analysis. LSR velocities are in km s^{-1}. **c)** Cut across the two clouds in velocity space with start and end points denoted by v1a/b and v2a/b for clouds S and N respectively.

are near-constant velocities apart from in its centre. At comparable resolution, such gradients as seen in cloud S have been observed before, for example in HVC 114–10–440 (Cohen & Mirabel 1979), which additionally showed a two-component velocity structure that was later found to be the result of beam-smearing of the velocity gradient (Wakker & Schwarz 1991). The observed gradient in M 92 S is much lower than has been seen in some HVC cores, that can reach 100 km s^{-1} degree^{-1} (Wakker & van Woerden 1997), although similar to the observed gradient in Complex H of ∼15 km s^{-1} degree^{-1} (Morras et al. 1998). The velocity gradient across cloud S could be caused by cloud rotation, although the cloud itself is unlikely to be gravitationally bound, at least in the absence of dark matter and assuming a distance of ∼10 kpc.

The second difference between the clouds is their orientation with respect to the Galactic plane. Cloud N is roughly aligned with the plane, with Cloud S lying perpendicular to it.

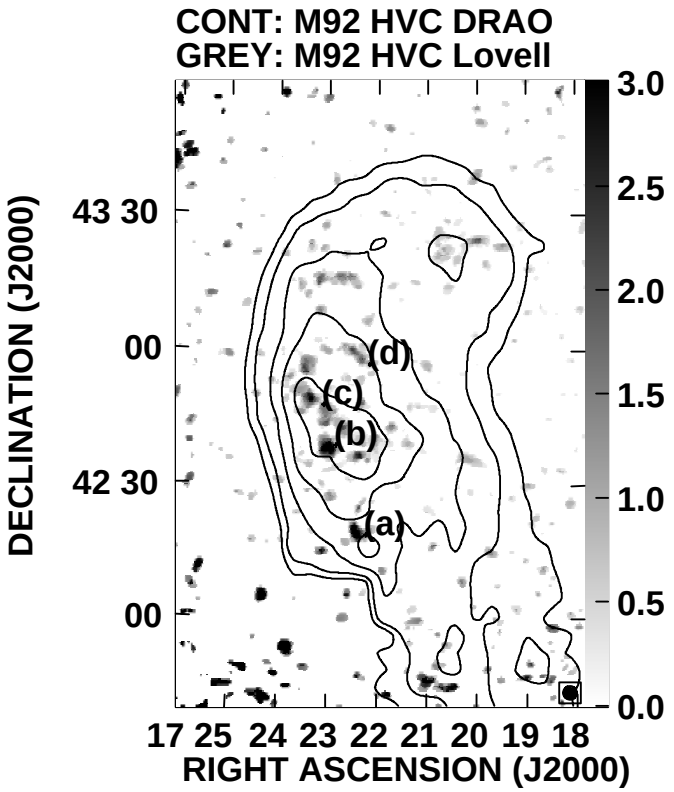

Fig. 10. M 92 HVC northern component. Greyscale: H I column density integrated between –120 km s^{-1} and –85 km s^{-1} observed with the DRAO synthesis telescope, convolved to a resolution of 3 arcmin and corrected for primary beam attenuation. Greyscale is from 0–3×10^{19} cm^{-2}. Contours: Corresponding Lovell telescope H I data at $N_{\rm HI}$ = (0.5, 1, 2, 3, 4)×10^{19} cm^{-2}. The DRAO-measured H I clouds are marked (a)–(d).

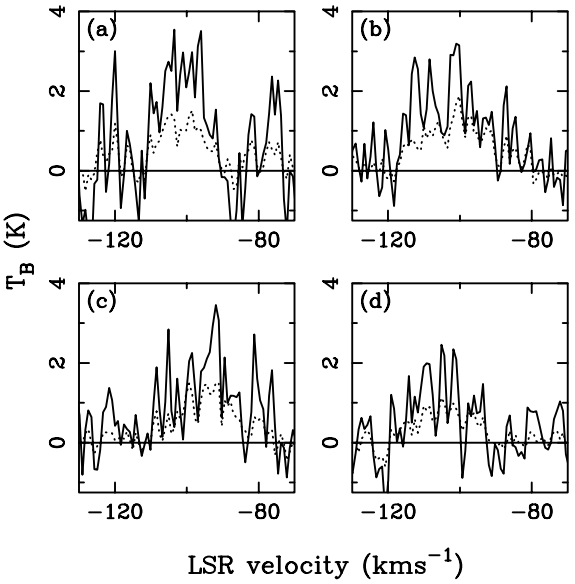

Fig. 11. Brightness temperature H I spectra of the four peaks in column density observed with the DRAO synthesis telescope at a resolution of 3 arcmin (solid line) and 6 arcmin (dotted line) and marked in Fig. 10. The data have been corrected for primary beam attenuation.

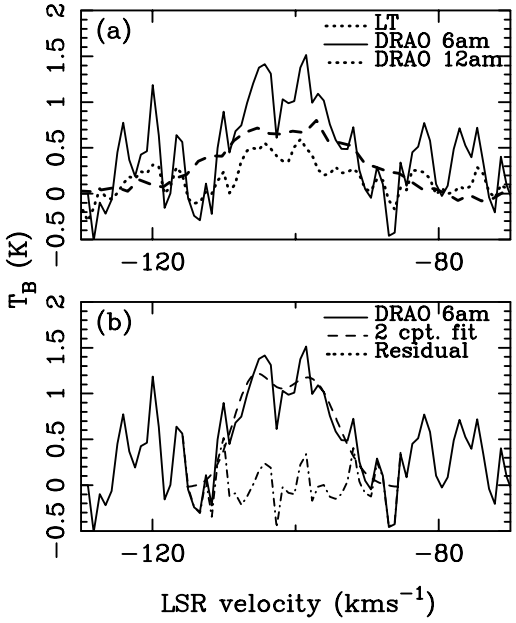

Fig. 12. Brightness temperature H I spectra towards region "a" in the Northern M 92 HVC cloud marked in Fig. 10. **a)** Lovell telescope and DRAO H I spectra, smoothed to resolutions of 6 and 12 arcmin. **b)** DRAO spectrum, smoothed to 6 arcmin resolution, overlaid with a two-component Gaussian fit and (data-fit) residual.

5. Summary and conclusions

We have conducted H I observations at spatial resolutions of 3 and 12 arcmin towards part of the HVC Complex C in the general direction of the M 92 globular cluster. The lower resolution data give results very similar to other observations of Northern Hemisphere HVCs, with a peak H I column density in the region of 5×10^{19} cm^{-2} and FWHM velocity widths at 12 arcmin resolution of ∼22 km s^{-1}. The DRAO observations are the first high spatial resolution data to be taken towards a part of Complex C. At a resolution of 3 arcmin these also show broad velocity widths, although smoothing to a spatial resolution of 6 arcmin indicates that the N cloud may have two velocity components with FWHM widths of 5–7 km s^{-1}.

Future observations towards this cloud should include high-resolution synthesis mapping towards the southern cloud in order to probe the finer scale structure, possible rotational properties and two-component velocity structure. Additionally, long H I integrations towards a strip through the cloud would be useful in order to probe the falloff in H I gas density. Combined with Hα mapping of the cloud (parts of which are known to be ionised; Tufte et al. 1998), this would provide information about the ionisation structure of the object and the change in relative neutral-to-ionised content with distance from the cloud centre. Furthermore, such sensitive observations would

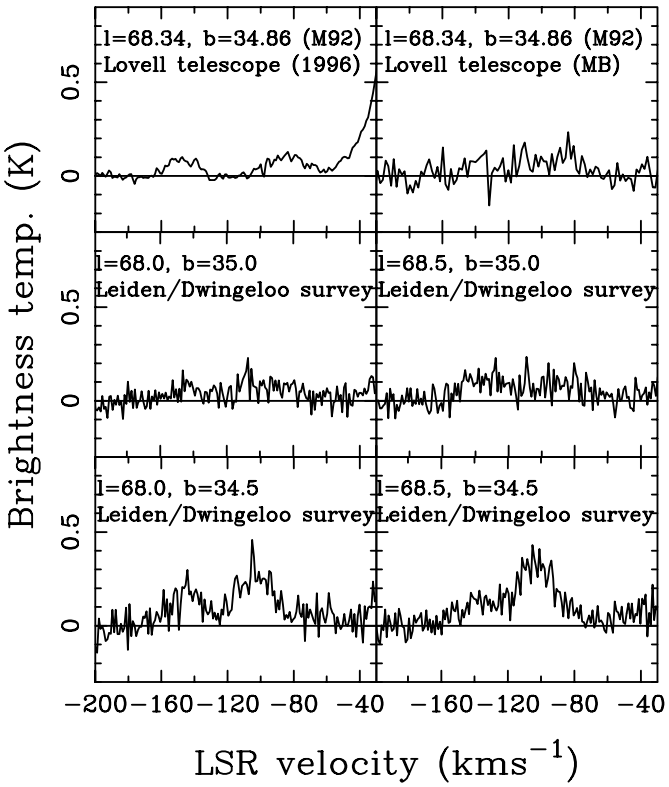

Fig. 13. Brightness temperature H I spectra in the vicinity of the M 92 globular cluster, displaying the 1996 single-beam Lovell telescope observations, the current multibeam results, and the nearest four positions taken from the Leiden/Dwingeloo survey.

provide evidence whether there are bridges between IVCs and HVCs in this part of Complex C, as have been observed by Pietz et al. (1996).

Acknowledgements. We would like to thank Chris Jordan at Jodrell Bank for her extensive help with the Lovell telescope observations, also to Peter Boyce and Robert Minchin for advice concerning the multibeam software and trips to the Crown. Thanks to Robert Ryans and Dave Kennedy for supplying us with 1996 Lovell telescope results. JVS is grateful for hospitality from both DRAO and Jodrell Bank and also thanks PPARC for financial support. Thanks are due to the referee, Bart Wakker, for many useful corrections to the initial version of this paper. The Digitized Sky Surveys were produced at the Space Telescope Science Institute under U.S. Government grant NAG W-2166. IPAC is operated by the Jet Propulsion Laboratory (JPL) and California Institute of Technology (Caltech) for NASA. IPAC is funded by NASA as part of the IRAS extended mission program under contract to JPL/Caltech.

References

Allen, C. W. 1973, Astrophysical Quantities, 3rd edition (University of London, Athlone Press)
Andrews, S. M., Meyer, D. M., & Lauroesch, J. T. 2001, ApJ, 552, 73
Barnes, D. G., Staveley-Smith, L., de Blok, W. J. G., et al. 2001, MNRAS, 322, 486
Beers, T. C. 1990, AJ, 99, 323
Blitz, L., Spergel, D. N., Teuben, P. J., Hartmann, D., & Burton, W. B 1999, ApJ, 514, 818
Boulanger, F., Abergel, A., Bernard, J.-P., et al. 1996, A&A, 312, 256
Braun, R., & Burton, W. B. 2000, A&A, 354, 853
Carretta, E., Gratton, R. G., Clementini, G., & Fusi Pecci, F. 2000, ApJ, 533, 215
Cohen, R. J., & Mirabel, I. F. 1979, MNRAS, 186, 217
Davies, R. D. 1975, MNRAS, 170, 45P
Davies, R. D., Buhl, D., & Jafolla, J. 1976, A&AS, 23, 181
Giovanelli, R., Verschuur, G. L., & Cram, T. R. 1973, A&AS, 12, 209
Greenstein, J. L. 1968, ApJ, 152, 431
Hartmann, D., & Burton W. B. 1997, Atlas of galactic neutral hydrogen (Cambridge University Press)
Heiles, C. 1997, ApJ, 481, 193
Howarth, I. D., Murray, J., Mills, D., & Berry, D. S. 1996, STARLINK, User Note SUN 50 (Rutherford Appleton Laboratory/CCLRC)
Hulsbosch, A. N. M. 1975, A&A, 40, 1
Hulsbosch, A. N. M., & Wakker, B. P. 1988, A&AS, 75, 191
Jaschek, C., & Jaschek, M. 1987, The classification of stars (Cambridge University Press)
Kalberla, P. M. W., Mebold, U., & Reif, K. 1982, A&A, 106, 190
Kennedy, D. C., Bates, B., Keenan, F. P., et al. 1998, MNRAS, 297, 849
Kerr, F. J., & Knapp, G. R. 1972, AJ, 77, 354 (KK72)
Langer, G. E., Prosser, C. F., & Sneden, C. 1990, AJ, 100, 216
Landecker, T. L., Dewdney, P. E., Burgess, T. A., et al. 2000, A&AS, 145, 509
Lynden-Bell, D. 1976, MNRAS, 174, 695
Mirabel, I. F. 1982, ApJ, 256, 112
Morras, R., Bajaja, E., & Arnal, E. M. 1998, A&A, 334, 659
Münch, G., & Zirin, H. 1961, ApJ, 133, 11
Pietz, J., Kerp, J., Kalberla, P. M. W., et al. 1996, A&A, 308, 37
Schwarz, U. J., & Oort, J. H. 1981, A&A, 101, 305
Shatsova, R. B. 1983, Afz, 19, 779
Shaw, C. R., Bates, B., Kemp, S. N., et al. 1996, ApJ, 473, 849
Smoker, J. V., Lehner, N., Keenan, F. P., et al. 2001, MNRAS, 322, 13
Tufte, S. L., Reynolds, R. J., & Haffner, L. M. 1998, ApJ, 504, 773
van Woerden, H., Schwarz, U. J.., Peletier, R. F., Wakker, B. P., & Kalberla, P. M. W. 1999a, Nature, 400, 138
van Woerden, H., Peletier, R. F., Schwarz, U. J., Wakker, B. P., & Kalberla, P. M. W. 1999, in Stromlo Workshop on High-Velocity Clouds, ed. Gibson, B. K., & Putman, M. E., ASP Conf. Ser., 166, 1
Wakker, B. P., & Boulanger, F. 1986, A&A, 170, 84
Wakker, B. P., & Schwarz, U. J. 1991, A&A, 250, 484
Wakker, B. P., & van Woerden, H. 1991, A&A, 250, 509
Wakker, B. P., & van Woerden, H. 1997, ARA&A, 35, 217
Wakker, B., van Woerden, H., de Boer, K. S., & Kalberla, P. 1998, ApJ, 493, 762
Wakker, B. P., Howk, J. C., Savage, B. D., et al. 1999, A&AS, 194, 4604 (abstr.)
Wallace, P., Clayton, C. 1996, RV, STARLINK, User Note SUN 78 (Rutherford Appleton Laboratory/CCLRC)